

A gold nanoparticle conjugate with photosystem I and photosystem II for development of a biohybrid water-splitting photocatalyst

Kousuke Kawahara ^a, Natsuko Inoue-Kahino ^b, Keisuke Namie ^c, Yuki Kato ^a, Tatsuya Tomo ^d, Yutaka Shibata ^c, Yasuhiro Kashino ^b and Takumi Noguchi ^{a,*}

^a *Division of Material Science, Graduate School of Science, Nagoya University, Furo-cho, Chikusa-ku, Nagoya, 464-8602, Japan*

^b *Department of Life Science, University of Hyogo, 3-2-1 Kohto, Kamigohri, Ako-gun, Hyogo 678-1297, Japan*

^c *Department of Chemistry, Graduate School of Science, Tohoku University, Aramaki Aza Aoba, Aoba-Ku, Sendai 980-8578, Japan*

^d *Faculty of Science, Tokyo University of Science, Tokyo 162-8601, Japan*

Abstract. Cyanobacterial photosystem I (PSI) and photosystem II (PSII) complexes were assembled on a gold nanoparticle (GNP) to generate a biohybrid photocatalyst. Optical absorption and fluorescence measurements of the generated GNP conjugates showed signals from both PSI and PSII. Moreover, single-particle fluorescence analysis using a cryogenic microscopy provided definitive evidence that both PSI and PSII complexes are bound together to a single GNP. This PSI-GNP-PSII conjugate will be a useful platform for further development of a water-splitting nanodevice for hydrogen production using solar energy.

Keywords: Artificial photosynthesis, gold nanoparticle, photosystem, single-particle fluorescence

1. Introduction

Usage of solar energy is an ultimate solution for the energy and environmental crisis that we face today. For this purpose, the development of efficient artificial photosynthetic systems, which convert solar energy to fuels as chemical energy, is urgent [4,13,25]. One of the most attractive systems is a water-splitting photocatalyst that produces hydrogen from water using solar energy [1,21,25]. Here, two photocatalysts for oxygen and hydrogen production are often combined to utilize visible light [1,12], in analogy with the Z-scheme in natural photosynthesis, in which photosystem II (PSII) and photosystem I (PSI) function as an anode for water oxidation and a cathode for NADP⁺ reduction, respectively. In the development of such artificial photosynthetic systems, the bottleneck has been that of efficient photocatalysts of water oxidation [9,33]. An intriguing approach is utilizing PSII, which has a high

*Corresponding author. E-mail: tnoguchi@bio.phys.nagoya-u.ac.jp.

quantum efficiency (>0.9 [24]) in water oxidation, in combination with synthetic materials to construct semi-artificial photosynthetic systems [2,10,15,22,27,30,34,35].

In this context, we previously developed a biohybrid nanodevice, in which PSII core complexes from a thermophilic cyanobacterium were assembled on a gold nanoparticle (GNP) with a 20 nm diameter, as a water-oxidation anode in semi-artificial photosynthesis [19]. Dimeric PSII complexes were bound to a GNP through a (His)₆-tag attached to the electron-acceptor side and Ni-nitrilotriacetic acid (Ni-NTA) assembled on the GNP surface. It was shown that four to five PSII dimers were attached to a single GNP retaining oxygen evolution activity [19]. The optical property of this PSII-GNP conjugate was further analyzed using time-resolved fluorescence measurement, showing that the decays of picosecond components in PSII were accelerated and a nanosecond-decay component was lost upon binding to GNP [26].

Meanwhile, as a cathode in semi-artificial photosynthesis, PSI complexes have been utilized for light-driven hydrogen production by combining with platinum nanoparticles (PtNPs) [3,6,14,16,17,29,31,36]. In these systems, however, electrons are needed to be donated from sacrificial reagents. Thus, to complete a biohybrid water-splitting system that produces hydrogen from water using light energy, it is necessary to combine the anode and cathode devices using PSII and PSI, respectively.

In this study, we assembled cyanobacterial PSI and PSII complexes together on a GNP to generate a PSI-GNP-PSII conjugate, aiming at the development of such a water-splitting nanosystem. The generated PSI-GNP-PSII conjugates were analyzed by single-particle fluorescence measurement using a cryogenic microscope as well as conventional visible absorption and fluorescence measurements.

2. Materials and methods

2.1. Preparation of photosystem II and photosystem I complexes

PSII core complexes from *Thermosynechococcus elongatus*, in which the C-terminus of the CP47 subunit was (His)₆-tagged [5], were isolated using Ni²⁺ affinity column chromatography as reported previously [18].

In PSI of *Synechocystis* sp. PCC 6803, a (His)₆ tag was genetically introduced to the C-terminus of the PsaL subunit with the following method. A plasmid construct carrying a Km^r cartridge [20] was created by fusing four DNA fragments (Fragments 1–4) using In-Fusion (Takara). Fragment 1 (659 bp), which involves the genetic region of *psaL* with an additional (His)₆ sequence, and Fragment 2 (630 bp) with a downstream region of the *psaL* gene were cloned from the *Synechocystis* sp. PCC 6803 genome using two pairs of PCR primers, P1/P2 and P3/P4, respectively.

P1: 5'-CCGCCATGGCCGCGGGGAGGTCAATAAACTTAATG-3'

P2: 5'-ACAACGTGGCTTTCCTTAgtggtgatggtgatggtGTTAAATAGACCCCGGAAAATC-3'
(sequence of the (His)₆ tag is shown in lowercase)

P3: 5'-GCAGACCTCAGCGCCTAAATAACCTTATAACCTTTAAAC-3'

P4: 5'-ACGCGTTGGGAGCTCAAGCTGGGCCGTCCCTGG-3'.

For cloning of Fragment 3 (1216 bp) containing the Km^r cartridge from pUK4k (Amersham Pharmacia Biotech) and Fragment 4 (2959 bp) from pGEM-5Zf(+) (Promega), PCR primers, P5/P6 and P7/P8, respectively, were used.

P5: 5'-GGAAAGCCACGTTGTGTCTCAAATCTCTG-3'

P6: 5'-GGCGCTGAGGTCTGCCTCGTGAAGAAGGTG-3'

P7: 5'-CCGCGGCCATGGCGGCCGGGAGCATGCGAC-3'

P8: 5'-GAGCTCCCAACGCGTTGGATGCATAGCTTG-3'.

Fragments 1, 3, and 2 were inserted into Fragment 4 in this order. The accuracy of PCR products was checked by sequencing. Transformation of *Synechocystis* sp. PCC 6803 was performed by a common procedure [32] and complete segregation of the mutations was confirmed by PCR.

(His)₆-tagged PSI complexes from this *Synechocystis* mutant were isolated using Ni²⁺ affinity column chromatography with a similar method to the preparation of the (His)₆-tagged PSII complexes.

2.2. Generation of a PSI-GNP-PSII conjugate

PSI and PSII complexes were assembled on the surface of a GNP by modifying the method of preparation of a PSII-GNP conjugate [19,26]. An aqueous solution (final 1.16 nM) of GNP with a 20-nm diameter (British Biocell International) was mixed with 3,3'-dithiobis[*N*-(5-amino-5-carboxypentyl)propionamide-*N'*, *N'*-diacetic acid] dihydrochloride (dithiobis(C₂-NTA)) (final 0.1 mM) and 0.06% *n*-dodecyl- β -D-maltoside (DM), and the obtained C₂-NTA-GNP was washed twice with 10 mM NaH₂PO₄/NaOH buffer (pH 7.0) containing 0.06% DM (buffer A) by centrifugation (11,900× *g*, 30 min, 4°C). The C₂-NTA-GNP was then suspended in buffer A in the presence of 30 μ M NiCl₂ to obtain Ni-NTA-GNP, which was washed with buffer A by centrifugation (6,000× *g*, 60 min, 4°C). A 1:1 mixture of the (His)₆-tagged PSI and PSII complexes was added to the Ni-NTA-GNP solution (PSI/II: GNP = 50: 1). The obtained PSI-GNP-PSII conjugates were washed twice with buffer A by centrifugation (6,000× *g*, 60 min, 4°C).

2.3. Absorption and fluorescence measurements

Visible absorption spectra were measured at room temperature using a Shimadzu UV-3100PC spectrophotometer at a 2 nm resolution. Fluorescence spectra were measured at 77 K using a JASCO FP-6500 fluorescence spectrophotometer with 430-nm excitation (5 nm resolution) at a fluorescence resolution of 1 nm. The sample for fluorescence measurement was mixed with glycerol (50% V/V) and placed in a glass tube with a diameter of 4 mm in a liquid-nitrogen dewar.

2.4. Single-particle fluorescence measurement

The fluorescence spectrum of a single PSI-GNP-PSII complex was measured with a laboratory-built cryogenic microscope as reported previously [7,23]. A PSI-GNP-PSII suspension (3.5 μ g Chl/mL) was diluted with a mixture of buffer A and glycerol (1:2) by a factor of 8000 (final concentration: 0.31 ng Chl/mL), and frozen at 90 K in a cryostat. A laser beam from a He-Ne laser (1137P, JDS Uniphase) passed through a filter (NT65-753, Edmund Optics) was reflected by a dichroic mirror and focused on the sample with a vacuum-compatible objective lens (Plan Apo HR100× NA0.9, Mitutoyo). Fluorescence from the sample was collected with the same objective lens and focused on the slit of a polychromator (MS2004i, SOL Instruments). A liquid N₂-cooled charge-coupled device (CCD) camera (PyLoN:100BR eXcelon, Princeton Instruments) was used as a detector.

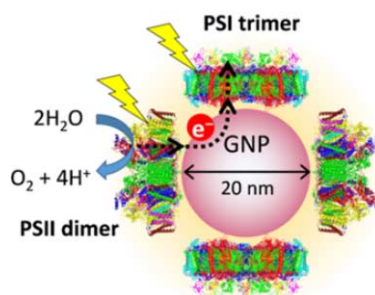


Fig. 1. Schematic view of a PSI-GNP-PSII conjugate designed in this study. The electron acceptor and donor sides of PSII and PSI complexes, respectively, are attached to a GNP through $(\text{His})_6$ tags and Ni-NTA, and thus electrons abstracted from H_2O in PSII are expected to be transferred to PSI upon illumination.

3. Results and discussion

We designed a PSI-GNP-PSII conjugate so that upon light irradiation, electrons abstracted from water at the Mn_4CaO_5 cluster in PSII are transferred to its quinone electron acceptors and then to P700 of PSI, ideally, via GNP, further to the Fe-S centers on its electron acceptor side (Fig. 1). Thus, the $(\text{His})_6$ tags were introduced to the C-terminus of the CP47 subunit on the electron acceptor side of PSII and that of the PsaL subunit on the electron donor side of PSI. PSI and PSII complexes were then immobilized on a GNP via the binding of the $(\text{His})_6$ tags with Ni-NTA attached to the GNP surface. PSI and PSII complexes of cyanobacteria usually exist in a trimer [8] and a dimer [28], respectively, and hence they are considered to be bound to a GNP in such multimeric forms.

The absorption spectrum of the obtained PSI-GNP-PSII conjugates (Fig. 2A, red line) showed a large band at 530 nm due to the surface plasmon absorption of GNP and small bands at 678 nm and 438 nm arising from the Q_y and Soret transitions of chlorophyll (Chl) *a*. This GNP band at 530 nm was slightly red-shifted compared with the corresponding band of Ni-NTA-GNP at 528 nm (Fig. 2A, black line), which has also been observed in our previous study of the generation of PSII-GNP conjugates that showed a GNP band at 533 nm [19,26]. This observation thus supports the binding of proteins on the surface of a GNP. In addition, the Q_y and Soret bands in the PSI-GNP-PSII conjugates (678 and 438 nm) were found between those of free PSII (674 and 436 nm) and PSI (680 and 439 nm) complexes in solution (Fig. 2A, B, blue and green lines). Because the PSII-GNP conjugates previously showed the same Q_y and Soret positions as those of free PSII [19,26], the above observation suggests that both PSI and PSII complexes are bound to GNPs.

The fluorescence spectrum of the PSI-GNP-PSII conjugates at 77 K (Fig. 3, red line) showed two bands at 686 and 718 nm. The former and latter bands correspond to the fluorescence bands of free PSII and PSI at 685 and 720 nm, respectively (Fig. 3, blue and green lines, respectively). Although free PSII showed distinct two peaks at 685 and 693 nm, the longer-wavelength peak was lost in the PSI-GNP-PSII conjugates. This observation is in agreement with the previous observation of the PSII-GNP conjugates, in which the 693-nm peak was lost and only a single peak at 683 nm was detected in its fluorescence spectrum at 77 K [26]. The 693-nm component was also absent in time-resolved fluorescence measurement of PSII-GNP, and hence this phenomenon was attributed to the structural perturbation of the 'red Chl' by the interaction with GNP rather than faster quenching of fluorescence [26]. The same observation in the PSI-GNP-PSII conjugates indicates that the interaction of PSII with the GNP surface was not affected by further binding of PSI, which probably replaced some of the PSII

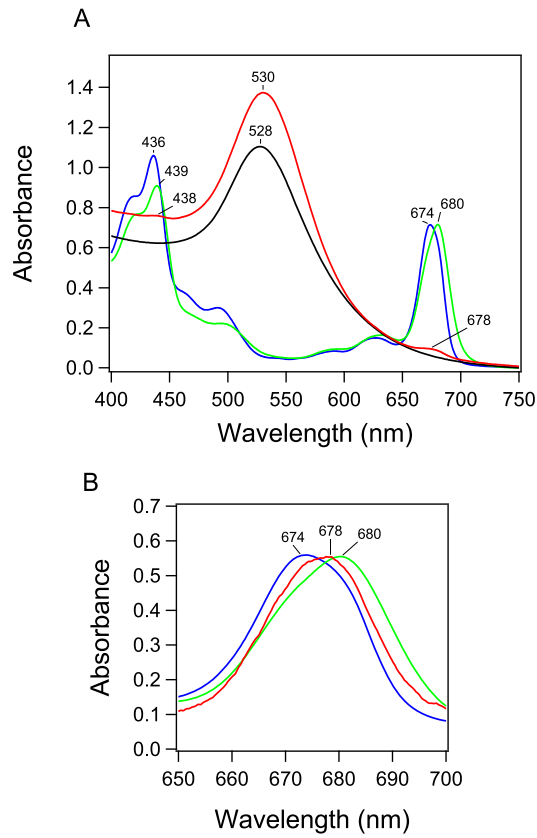


Fig. 2. (A) Absorption spectrum of PSI-GNP-PSII conjugates (red line) in comparison with the spectra of Ni-NTA-GNP (black line), and free PSI (green line) and PSII (blue line) complexes. (B) Expanded view of the Chl Q_y band of the PSI-GNP-PSII conjugates after baseline correction (red line) in comparison with the Q_y bands of free PSI (green line) and PSII (blue line) complexes. The three spectra were normalized by the intensities of the Q_y bands.

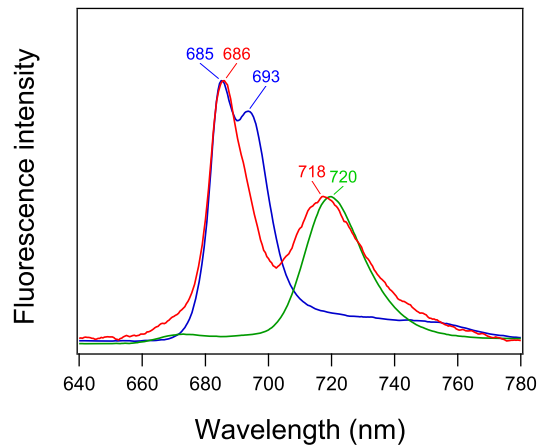


Fig. 3. Fluorescence spectrum of PSI-GNP-PSII conjugates (red line) in comparison with the spectra of free PSI (green line) and PSII (blue line) complexes measured at 77 K. The spectra of free PSI and PSII were normalized to the spectrum of PSI-GNP-PSII at the corresponding maximum peaks.

complexes in a PSII-GNP conjugate. In contrast to PSII, the fluorescence band of PSI at 718 nm in PSI-GNP-PSII showed no significant change from the fluorescence band of free PSI at 720 nm except for a slight blue shift with a broader width (Fig. 3). This observation indicates that the interaction of PSI with GNP little affects its fluorescence property, although there is some heterogeneity in the PSI complexes bound to GNP.

The fluorescence spectrum of the PSI-GNP-PSII conjugates shown in Fig. 3 (red line) originates from the ensemble of a large number of nanoparticles in solution. Thus, the possibility cannot be excluded that the sample solution is actually the mixture of the PSII-GNP and PSI-GNP conjugates. We therefore further detected fluorescence from a single nanoparticle by single-particle fluorescence measurement using a cryogenic microscope, which has lateral and axial resolutions of 0.39 and 1.3 μm , respectively [23]. The sample was diluted enough (0.31 ng Chl/mL) and frozen at 90 K. Our previous study showed that a PSII-GNP conjugate attached ~ 4.7 PSII dimers on average on one GNP [19]. Assuming that three PSII dimers and two PSI trimers are attached in a PSI-GNP-PSII conjugate, this concentration corresponds to 0.62 pM GNP and hence to about 14- μm separation between particles, which is large enough to separately detect each GNP conjugate with the above spatial resolution. The fluorescence microscope images of two particles are selected and shown in Fig. 4A(a, b). The size of each image is similar to the spatial resolution of the microscope, confirming that we indeed detected a single GNP complex in each fluorescence image.

The fluorescence spectra of the images a and b (Fig. 4Ba, b) showed prominent two peaks corresponding to the PSII and PSI bands at 686 and 718 nm, respectively, in the fluorescence spectrum of the ensemble of the PSI-GNP-PSII conjugates (Fig. 4Bc). The peak positions were slightly different between the two PSI-GNP-PSII conjugates, reflecting some differences in the interactions of ‘red Chls’ that emit fluorescence in the PSI and PSII proteins frozen at a cryogenic temperature. In addition, the relative intensities of the PSII and PSI bands were different between the two particles. This may simply indicate that there is some variation in the numbers of the PSI and PSII complexes attached to a GNP. Alternatively, time-dependent fluctuation of the fluorescence intensity, so-called ‘blinking’ [7,11], could also contribute to this change in the relative intensity of the PSI and PSII bands. The presence of both the PSI and PSII bands in the microscopic fluorescence spectra of separate particles of the PSI-GNP-PSII

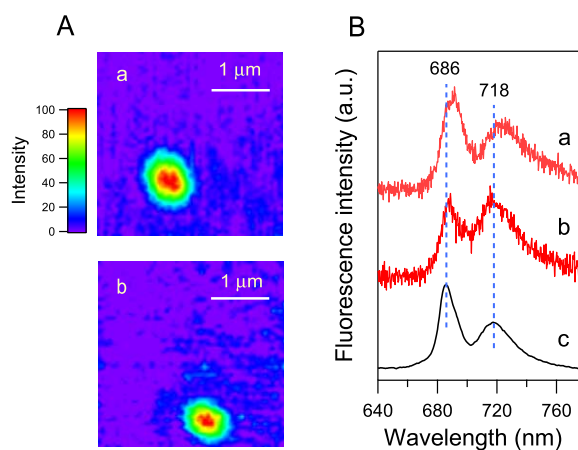


Fig. 4. (A) Fluorescence microscope image of a single PSI-GNP-PSII conjugate at 90 K. The images of two particles (a, b) are shown. (B) Microscopic fluorescence spectra (a, b) corresponding to the two images in panel Aa, b in comparison with the macroscopic fluorescence spectrum of PSI-GNP-PSII conjugates at 77 K (c; identical to Fig. 3, red line).

conjugate (Fig. 4B), along with the PSI and PSII signals in the macroscopic absorption (Fig. 2, red line) and fluorescence (Fig. 3, red line) spectra, provided definitive evidence that the PSI and PSII complexes are bound together to the same GNP and the designed PSI-GNP-PSII conjugate (Fig. 1) was successfully generated.

4. Conclusions

We have assembled cyanobacterial PSI and PSII complexes on a GNP, aiming at the development of an efficient semi-artificial photosynthesis system. The generated GNP conjugate was analyzed by single-particle fluorescence measurement at a cryogenic temperature as well as conventional optical absorption and fluorescence measurements, providing definitive evidence that both the PSI and PSII complexes are bound together on a single GNP. We previously showed that PSII core complexes retained the O₂ evolving activity in PSII-GNP conjugates, in which the PSII complexes are bound to GNPs on the electron-acceptor side [19]. Also, it has been reported that PSI complexes can evolve hydrogen upon irradiation using electrons from sacrificial electron donors when they are coupled to PtNPs [3,6,14,16,17,29,31,36]. Thus, the PSI-GNP-PSII conjugate that we generated in the present study can be a useful platform for further development of a light-driven water-splitting nanodevice for production of hydrogen from water using solar energy.

Acknowledgements

The authors thank Dr. Hanayo Ueoka-Nakanishi for technical assistance in sample preparations. This study was supported by JSPS KAKENHI Grant Number JP19H02674 (to Yu.K.), JP26220801, JP17K07453, JP18H05177, JP19H03187 (to T.T.), JP24370060 (to Y.S.), JP23570063 (to Ya.K.), JP17H06435, JP17H03662, and JP17H06433 (to T.N.).

Conflict of interest

The authors have no conflict of interest to report.

References

- [1] R. Abe, Recent progress on photocatalytic and photoelectrochemical water splitting under visible light irradiation, *J. Photochem. Photobiol. C* **11**(4) (2010), 179–209. doi:10.1016/j.jphotochemrev.2011.02.003.
- [2] A. Badura, B. Esper, K. Ataka, C. Grunwald, C. Wöll, J. Kuhlmann, J. Heberle and M. Rögner, Light-driven water splitting for (bio-)hydrogen production: Photosystem 2 as the central part of a bioelectrochemical device, *Photochem. Photobiol.* **82**(5) (2006), 1385–1390. doi:10.1562/2006-07-14-RC-969.
- [3] R.A. Grimme, C.E. Lubner, D.A. Bryant and J.H. Golbeck, Photosystem I/molecular wire/metal nanoparticle bioconjugates for the photocatalytic production of H₂, *J. Am. Chem. Soc.* **130**(20) (2008), 6308–6309. doi:10.1021/ja800923y.
- [4] D. Gust, T.A. Moore and A.L. Moore, Solar fuels via artificial photosynthesis, *Acc. Chem. Res.* **42**(12) (2009), 1890–1898. doi:10.1021/ar900209b.
- [5] M. Iwai, T. Suzuki, A. Kamiyama, I. Sakurai, N. Dohmae, Y. Inoue and M. Ikeuchi, The PsbK subunit is required for the stable assembly and stability of other small subunits in the PSII complex in the thermophilic cyanobacterium *Thermosynechococcus elongatus* BP-1, *Plant Cell Physiol.* **51**(4) (2010), 554–560. doi:10.1093/pcp/pcq020.
- [6] I.J. Iwuchukwu, M. Vaughn, N. Myers, H. O'Neill, P. Frymier and B.D. Bruce, Self-organized photosynthetic nanoparticle for cell-free hydrogen production, *Nat. Nanotechnol.* **5**(1) (2010), 73–79. doi:10.1038/nnano.2009.315.

- [7] S. Jana, T. Du, R. Nagao, T. Noguchi and Y. Shibata, Redox-state dependent blinking of single photosystem I trimers at around liquid-nitrogen temperature, *Biochim. Biophys. Acta* **1860**(1) (2019), 30–40. doi:10.1016/j.bbabi.2018.11.002.
- [8] P. Jordan, P. Fromme, H.T. Witt, O. Klukas, W. Saenger and N. Krauß, Three-dimensional structure of cyanobacterial photosystem I at 2.5 Å resolution, *Nature* **411**(6840) (2001), 909–917. doi:10.1038/35082000.
- [9] K.S. Joya and H.J.M. de Groot, Biomimetic molecular water splitting catalysts for hydrogen generation, *Int. J. Hydrogen Energy* **37**(10) (2012), 8787–8799. doi:10.1016/j.ijhydene.2012.01.139.
- [10] M. Kato, T. Cardona, A.W. Rutherford and E. Reisner, Covalent immobilization of oriented photosystem II on a nanostructured electrode for solar water oxidation, *J. Am. Chem. Soc.* **135**(29) (2013), 10610–10613. doi:10.1021/ja404699h.
- [11] T.P.J. Krüger, C. Illoiaia and R. van Grondelle, Fluorescence intermittency from the main plant light-harvesting complex: Resolving shifts between intensity levels, *J. Phys. Chem. B* **115**(18) (2011), 5071–5082. doi:10.1021/jp201609c.
- [12] K. Maeda, Z-scheme water splitting using two different semiconductor photocatalysts, *ACS Catal.* **3**(7) (2013), 1486–1503. doi:10.1021/cs4002089.
- [13] I. McConnell, G.H. Li and G.W. Brudvig, Energy conversion in natural and artificial photosynthesis, *Chem. Biol.* **17**(5) (2010), 434–447.
- [14] J.F. Millsaps, B.D. Bruce, J.W. Lee and E. Greenbaum, Nanoscale photosynthesis: Photocatalytic production of hydrogen by platinumized photosystem I reaction centers, *Photochem. Photobiol.* **73**(6) (2001), 630–635. doi:10.1562/0031-8655(2001)073<0630:NPPPOH>2.0.CO;2.
- [15] M. Miyachi, S. Ikehira, D. Nishiori, Y. Yamanoi, M. Yamada, M. Iwai, T. Tomo, S.I. Allakhverdiev and H. Nishihara, Photocurrent generation of reconstituted photosystem II on a self-assembled gold film, *Langmuir* **33**(6) (2017), 1351–1358. doi:10.1021/acs.langmuir.6b03499.
- [16] M. Miyachi, K. Okuzono, D. Nishiori, Y. Yamanoi, T. Tomo, M. Iwai, S.I. Allakhverdiev and H. Nishihara, A photochemical hydrogen evolution system combining cyanobacterial photosystem I and platinum nanoparticle-terminated molecular wires, *Chem. Lett.* **46**(10) (2017), 1479–1481. doi:10.1246/cl.170576.
- [17] H. Nagakawa, A. Takeuchi, Y. Takekuma, T. Noji, K. Kawakami, N. Kamiya, M. Nango, R. Furukawa and M. Nagata, Efficient hydrogen production using photosystem I enhanced by artificial light harvesting dye, *Photochem. Photobiol. Sci.* **18**(2) (2019), 309–313.
- [18] S. Nakamura, R. Nagao, R. Takahashi and T. Noguchi, Fourier transform infrared detection of a polarizable proton trapped between photooxidized tyrosine Y_Z and a coupled histidine in photosystem II: Relevance to the proton transfer mechanism of water oxidation, *Biochemistry* **53**(19) (2014), 3131–3144. doi:10.1021/bi500237y.
- [19] T. Noji, H. Suzuki, T. Gotoh, M. Iwai, M. Ikeuchi, T. Tomo and T. Noguchi, Photosystem II–gold nanoparticle conjugate as a nanodevice for the development of artificial light-driven water-splitting systems, *J. Phys. Chem. Lett.* **2**(19) (2011), 2448–2452. doi:10.1021/jz201172y.
- [20] A. Oka, H. Sugisaki and M. Takanami, Nucleotide sequence of the kanamycin resistance transposon Tn903, *J. Mol. Biol.* **147**(2) (1981), 217–226. doi:10.1016/0022-2836(81)90438-1.
- [21] F.E. Osterloh, Inorganic nanostructures for photoelectrochemical and photocatalytic water splitting, *Chem. Soc. Rev.* **42**(6) (2013), 2294–2320. doi:10.1039/C2CS35266D.
- [22] M. Riedel, J. Wersig, A. Ruff, W. Schuhmann, A. Zouni and F. Lisdat, A Z-scheme-inspired photobioelectrochemical H₂O/O₂ cell with a 1 V open-circuit voltage combining photosystem II and PbS quantum dots, *Angew. Chem. Int. Edit.* **58**(3) (2019), 801–805. doi:10.1002/anie.201811172.
- [23] Y. Shibata, W. Katoh, T. Chiba, K. Namie, N. Ohnishi, J. Minagawa, H. Nakanishi, T. Noguchi and H. Fukumura, Development of a novel cryogenic microscope with numerical aperture of 0.9 and its application to photosynthesis research, *Biochim. Biophys. Acta* **1837**(6) (2014), 880–887. doi:10.1016/j.bbabi.2014.03.006.
- [24] H. Suzuki, M. Sugiura and T. Noguchi, Determination of the miss probabilities of individual S-state transitions during photosynthetic water oxidation by monitoring electron flow in photosystem II using FTIR spectroscopy, *Biochemistry* **51**(34) (2012), 6776–6785. doi:10.1021/bi300708a.
- [25] Y. Tachibana, L. Vayssieres and J.R. Durrant, Artificial photosynthesis for solar water-splitting, *Nature Photonics* **6**(8) (2012), 511–518. doi:10.1038/nphoton.2012.175.
- [26] K. Tahara, A. Mohamed, K. Kawahara, R. Nagao, Y. Kato, H. Fukumura, Y. Shibata and T. Noguchi, Fluorescence property of photosystem II protein complexes bound to a gold nanoparticle, *Faraday Discuss.* **198** (2017), 121–134. doi:10.1039/C6FD00188B.
- [27] N. Terasaki, M. Iwai, N. Yamamoto, T. Hiraga, S. Yamada and Y. Inoue, Photocurrent generation properties of Histag-photosystem II immobilized on nanostructured gold electrode, *Thin Solid Films* **516**(9) (2008), 2553–2557.
- [28] Y. Umena, K. Kawakami, J.-R. Shen and N. Kamiya, Crystal structure of oxygen-evolving photosystem II at a resolution of 1.9 Å, *Nature* **473**(7345) (2011), 55–60.
- [29] L.M. Utschig, N.M. Dimitrijevic, O.G. Poluektov, S.D. Chemerisov, K.L. Mulfort and D.M. Tiede, Photocatalytic hydrogen production from noncovalent biohybrid photosystem I/Pt nanoparticle complexes, *J. Phys. Chem. Lett.* **2**(3) (2011), 236–241. doi:10.1021/jz101728v.

- [30] M. Vittadello, M.Y. Gorbunov, D.T. Mastrogiovanni, L.S. Wielunski, E.L. Garfunkel, F. Guerrero, D. Kirilovsky, M. Sugiura, A.W. Rutherford, A. Safari and P.G. Falkowski, Photoelectron generation by photosystem II core complexes tethered to gold surfaces, *ChemSusChem* **3**(4) (2010), 471–475. doi:[10.1002/cssc.200900255](https://doi.org/10.1002/cssc.200900255).
- [31] K.A. Walters and J.H. Golbeck, Designing a modified clostridial 2[4Fe-4S] ferredoxin as a redox coupler to directly link photosystem I with a Pt nanoparticle, *Photosynth. Res.* **143**(2) (2020), 165–181. doi:[10.1007/s11120-019-00679-w](https://doi.org/10.1007/s11120-019-00679-w).
- [32] J.G.K. Williams, Construction of specific mutations in photosystem II photosynthetic reaction center by genetic engineering methods in *Synechocystis* 6803, *Methods Enzymol.* **167** (1988), 766–778. doi:[10.1016/0076-6879\(88\)67088-1](https://doi.org/10.1016/0076-6879(88)67088-1).
- [33] L.L. Yang, H. Zhou, T.X. Fan and D. Zhang, Semiconductor photocatalysts for water oxidation: Current status and challenges, *Phys. Chem. Chem. Phys.* **16**(15) (2014), 6810–6826. doi:[10.1039/c4cp00246f](https://doi.org/10.1039/c4cp00246f).
- [34] O. Yehezkeli, R. Tel-Vered, J. Wasserman, A. Trifonov, D. Michaeli, R. Nechushtai and I. Willner, Integrated photosystem II-based photo-bioelectrochemical cells, *Nat. Commun.* **3** (2012).
- [35] J.Z. Zhang and E. Reisner, Advancing photosystem II photoelectrochemistry for semi-artificial photosynthesis, *Nat. Rev. Chem.* **4**(1) (2020), 6–21. doi:[10.1038/s41570-019-0149-4](https://doi.org/10.1038/s41570-019-0149-4).
- [36] F.Y. Zhao, F. Conzuelo, V. Hartmann, H.G. Li, M.M. Nowaczyk, N. Plumeré, M. Rögner and W. Schuhmann, Light induced H₂ evolution from a biophotocathode based on photosystem I-Pt nanoparticles complexes integrated in solvated redox polymers films, *J. Phys. Chem. B* **119**(43) (2015), 13726–13731. doi:[10.1021/acs.jpcc.5b03511](https://doi.org/10.1021/acs.jpcc.5b03511).